Enhanced Thermoelectric Performance of Single-Walled Carbon Nanotubes/Polyaniline Hybrid Nanocomposites

Qin Yao,[†,§] Lidong Chen,[†,*] Wenqing Zhang,[‡] Shengcong Liufu,[†] and Xihong Chen[†]

[†]CAS Key Laboratory of Materials for Energy Conversion, and [‡]State Key Laboratory of High Performance Ceramics and Superfine Microstructure, Shanghai Institute of Ceramics, Chinese Academy of Science, Shanghai 200050, China, and [§]Graduate University of Chinese Academy of Science, Beijing 100039, China

ABSTRACT Hybrid nanocomposites containing carbon nanotubes (CNTs) and ordered polyaniline (PANI) have been prepared through an *in situ* polymerization reaction using a single-walled nanotube (SWNT) as template and aniline as reactant. TEM, SEM, XRD, and Raman analyses show that the polyaniline grew along the surface of CNTs forming an ordered chain structure during the SWNT-directed polymerization process. The SWNT/PANI nanocomposites show both higher electrical conductivity and Seebeck coefficient as compared to pure PANI, which could be attributed to the enhanced carrier mobility in the ordered chain structures of the PANI. The maximum electrical conductivity and Seebeck coefficient of composites reach 1.25×10^4 S m^{-1} and 40 μV K^{-1}, respectively, and the maximum power factor is up to 2×10^{-5} W m^{-1} K^{-2}, more than 2 orders of magnitude higher than the pure polyaniline. This study suggests that constructing highly ordered chain structure is a novel and effective way for improving the thermoelectric properties of conducting polymers.

KEYWORDS: thermoelectric · carbon nanotubes · polyaniline · hybrid · nanocomposites

Thermoelectric (TE) materials have great potential for applications in both power generation and solid-state cooling or heating. The TE power generation could be widely used as a special power source and as novel energy harvesting systems, such as waste heat recovery and high efficiency solar energy conversion. Solid cooling/heating using TE technology has greatly contributed to developing frontier electronic devices.[1,2] However, the relatively high cost and poor processability of the state-of-the art inorganic semiconductor TE materials are impeding their spreading applications to many new TE systems.[3] It is timely and necessary to search for novel TE materials with high performance and low cost and to seek economical ways of manufacturing TE materials.

Compared with inorganic semiconductor materials, conducting polymers possess unique features for application as TE materials because of their low density, low cost due to rich resources, easy synthesis, and facile processing into versatile form. Furthermore, polymers inherently possess a low thermal conductivity, which offers them a significant advantage over conventional inorganic thermoelectric materials in terms of the performance of a thermoelectric material evaluated by its dimensionless figure of merit, $ZT = \alpha^2\sigma T/\kappa$ (α, σ, κ, and T are Seebeck coefficient, electrical conductivity, thermal conductivity, and absolute temperature, respectively). However, poor electrical transport properties of polymers, including low electrical conductivity (σ) and low Seebeck coefficient (α), have excluded them as feasible candidates for thermoelectric materials in the past. Up to now, the power factor ($\alpha^2\sigma$) for most polymer thermoelectric materials is in the range of 10^{-6}–10^{-10} W m^{-1} K^{-2}, 3 orders of magnitude less than that of the state-of-the-art inorganic TE materials.[4−10] In order to explore the feasibility of using polymers for TE materials, it is urgent to find an effective way to improve the power factor of conducting polymers.

In conventional semiconductors, the major parameters of thermoelectric transport are strongly correlated, making enhancement of ZT very difficult. For example, increasing electrical conductivity, if induced by increasing carrier concentration, usually results in a decrease of Seebeck coefficient, which obviously restrains the improvement of the power factor. Generally, improving carrier mobility is the most effective way to increase both electrical conductivity and Seebeck coefficient.[4−6,11,12] For most conducting polymers, carrier transport is principally controlled by the interchain and intrachain hopping processes and the transport

*Address correspondence to chenlidong@mail.sic.ac.cn.

Received for review February 7, 2010 and accepted March 25, 2010.

Published online April 1, 2010.
10.1021/nn1002562

behavior follows the variable range hopping (VRH) model.[13] The conformation and arrangement of polymer chains are critical to the carrier mobility. In general, an expanded chain conformation and an ordered chain arrangement would result in a reduced barrier of both interchain hopping and intrachain hopping and, therefore, enhance the carrier mobility.[4−6,14] It is considered to be vital to construct an ordered polymer structure for realizing high thermoelectric performance in conducting polymers.

Template-directed synthesis is one of the most effective means of producing 1D ordered nanostructures in which reactant materials are located within or in the immediate vicinity of the templates.[15] Many suitable nanoscale templates have been reported, such as mesoscale structures self-assembled from organic surfactants or block copolymers (soft templates),[16] existing nanostructures including step edges on solid surfaces,[17] biological DNA molecules, and rod-shaped viruses.[18] Carbon nanotubes (CNTs) are very special and often used as 1D hard templates for generating ordered nanomaterials because of their extremely stable 1D nanostructure and excellent electric and mechanical properties.[19,20] O'Connell and Balavoine reported that the ordering of chain structure for a few polymers has been improved by self-assembling them on the surface of CNTs by noncovalent interactions between the two components.[21,22] CNT/poly(vinyl acetate)(PVAc) and CNT/poly(3,4-ethlenedioxythiophene)poly(styrenesulfonate) (PEDOT:PSS) composite films with remarkably enhanced thermoelectric properties have also been reported by Yu *et al.*[7,23] Among the best-known conducting polymers, polyaniline (PANI) shows reasonably good electrical transport and is considered as one of the most promising TE materials because of its relatively facile processability, relatively good electrical conductivity, and environment stability. Moreover, it has been reported that there exist strong $\pi-\pi$ interactions between the CNTs' surfaces and polyaniline molecules,[24,25] which would benefit the growing of an ordered polyaniline chain along the surface of CNTs. In addition, CNTs fortunately show high dissolution in aniline solution,[26] which makes it possible to disperse CNTs in aniline reactant. Recently, Meng *et al.* found that multiwalled carbon nanotube (MWNT) sheet/PANI nanocomposites prepared by a two-step method showed enhanced thermoelectric properties, and the maximum power factor of their samples reached 5×10^{-6} W m^{-1} K^{-2}.[27]

Single-walled carbon nanotubes have more excellent electrical properties than multiwalled carbon nanotubes due to fewer structure defects in the SWNT. Herein, we prepared SWNT/PANI hybrid nanocomposites through a simple one-step *in situ* polymerization by using single-walled carbon nanotubes as templates and aniline as reactant. It was observed that the polyaniline tightly decorated the surface of SWNTs, forming nanocable structures. Both electrical conductivity and Seebeck coefficient of composites were greatly enhanced with increasing SWNT content. Furthermore, the carrier mobility, carrier density, and the chain structure of the composites were also investigated. It is found that the enhancement of thermoelectric properties for composites results from the enhanced carrier mobility in the ordered chain structures of the PANI induced by the interactions between SWNT and PANI. The composites exhibit relatively high thermoelectric properties. The maximum power factor is up to 2×10^{-5} W m^{-1} K^{-2}, which is more than 2 orders of magnitude higher than the pure polyaniline. Moreover, the addition of SWNTs did not result in a significant change of thermal conductivity and, therefore, resulted in a significant enhancement of ZT value.

RESULTS AND DISCUSSION

Figure 1 displays the typical TEM and SEM images of the SWNT/PANI powder containing 25 wt % SWNT. The composites show nanocable structures, in which a bundle of SWNTs was coated and bounded by PANI. The outer shell layer of polyaniline is 20−40 nm thick, and the core bundle of the SWNTs is about 30 nm in diameter. Along the length direction of the SWNT, most parts of the surface are tightly coated by PANI, and only a few parts of the SWNTs are naked (as shown by the arrows), implying strong binding between CNTs and PANI.

Figure 2 shows the room-temperature electrical transport properties of the composites as a function of SWNT content. The electrical conductivity of the 41.4 wt % SWNT sample reaches 1.25×10^4 S m^{-1}, which is more than 1 order of magnitude larger than the pure PANI. It is worth noting that the measured electrical conductivity value is also much higher than the calculated value based on the normal particle mixture rule. Furthermore, the Seebeck coefficient (α) shows great increase as the SWNT content is increased. The α value increased from 11 to 40 μV/K when the SWNT content changed from 0 to 41.4 wt %. The power factor at room temperature reaches 2×10^{-5} W m^{-1} K^{-2} for the 41.4 wt % SWNT sample, more than 2 orders of magnitude higher than the pure polyaniline.

The temperature dependence of electrical conductivity from 180 to 300 K has also been investigated, and the results are shown in Figure 3. As is known, the electrical conductivity of polyaniline usually follows the quasi-one-dimensional variable range hopping (1D-VRH) model:[13]

$$\sigma(T) = \sigma_0 \exp[T_0/T]^{1/2} \quad (2)$$

where σ_0 is a constant, T_0 is the characteristic Mott temperature that generally depends on the carrier hopping barriers. T_0 values are estimated by fitting eq 2 to the measured σ data. The fitted T_0, experimentally mea-

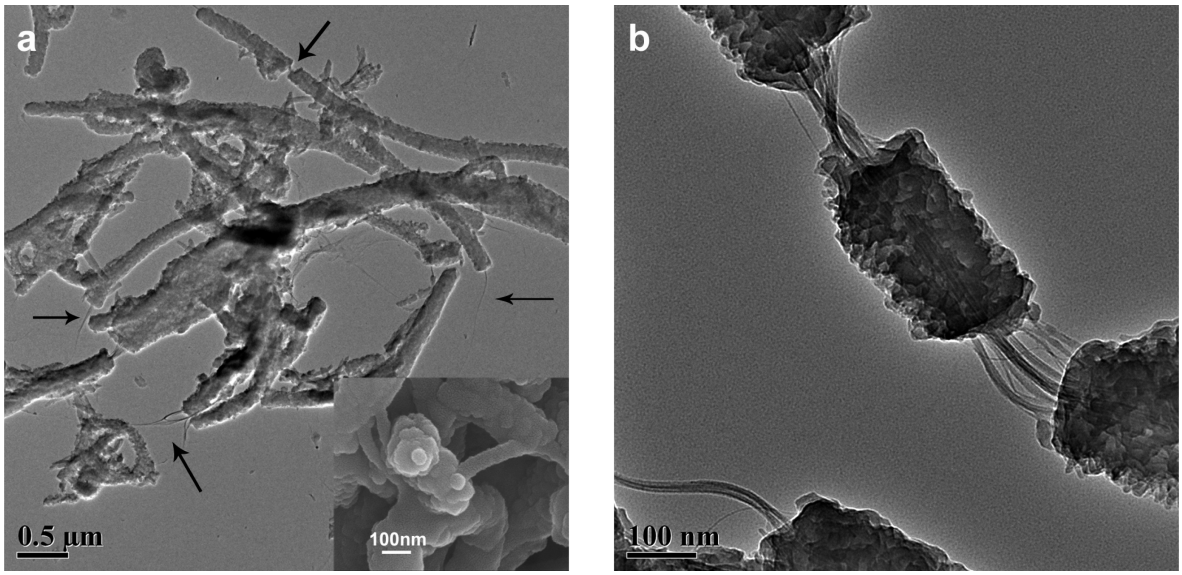

Figure 1. TEM images for SWNT/PANI composites with 25 wt % SWNT. Inset of (a) is the SEM top view of the nanocable.

sured carrier mobility, and carrier density are given in Table 1. It is observed that the T_0 decreases with increasing SWNT content, indicating that the carrier hopping barrier decreases with increasing SWNT content. It was also found that the carrier mobility of the composite dramatically increases while the carrier density does not change substantially with the increase of SWNT content. The improvement of electrical conductivity is considered to mainly come from the carrier mobility enhancement.

Recently, Meng *et al.* reported the CNT-based MWNT/PANI sheet composite and indicated that the improvement of thermoelectric properties for the composite should be attributed to the size-dependent energy-filtering effect caused by the nanostructured PANI coating layer enwrapped around the CNTs.[27] This should be one reasonable explanation for the enhanced thermoelectric performance of the CNT/PANI system in the present work. On the other hand, for the PANI-based composite, it is known that the electric transport properties are strongly dependent on the structure ordering of the polymer molecule.[4−6] The polyaniline molecule comprises benzene rings and quinoid rings, which are linked by an amine nitrogen atom. There exist strong π−π conjugated interactions between benzene rings and quinoid rings, acting as the channels of carrier transport. Generally, polyaniline exhibits the compacted coil conformation and random molecular arrangement. The π−π conjugated defects between rings caused by ring twisting usually lead to the decrease of carrier mobility and therefore degrade the electrical properties. The chain packing states (such as the ordering degree) are also expected to give great influence on the carrier mobility and electrical conductivity through adjusting the hopping barrier (including hopping free path and hopping active energy). Carbon

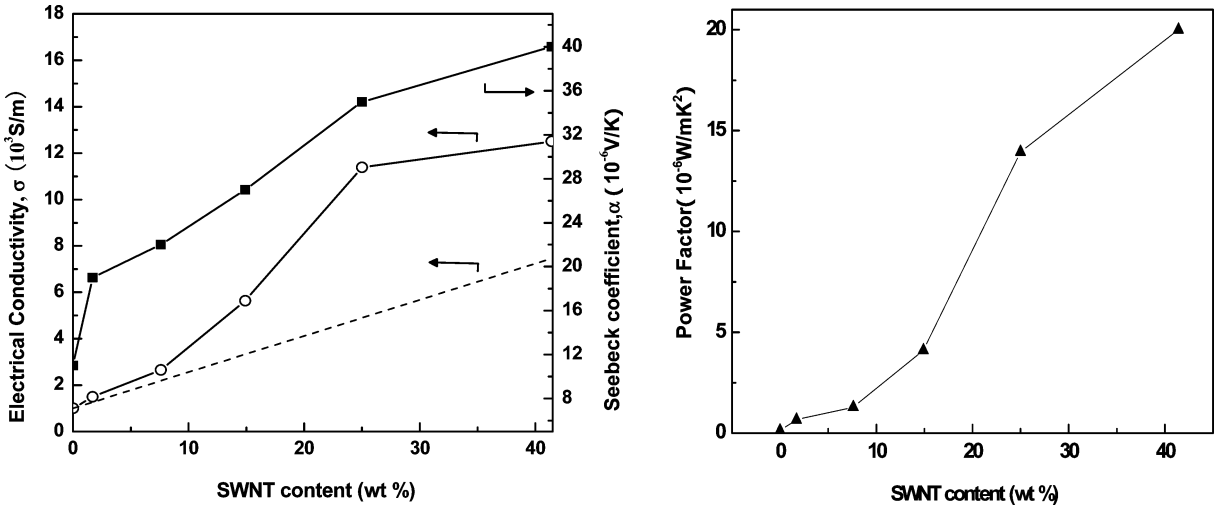

Figure 2. Seebeck coefficient (closed squares), electrical conductivity (open circles), and power factor (closed triangle) of SWNT/PANI composites with different SWNT content. The dashed line is the calculated electrical conductivity based on the particle mixture rule.

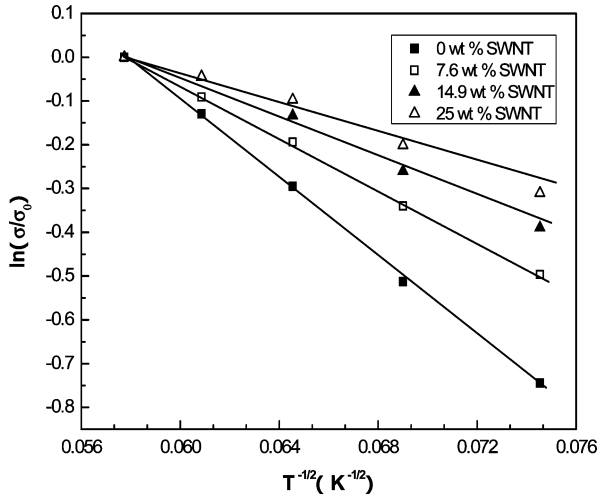

Figure 3. Temperature dependence of electrical conductivity for SWNT/PANI composites with different SWNT content; σ_0 is the electrical conductivity at 300 K.

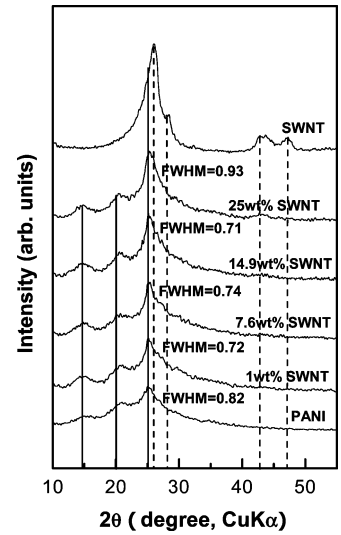

Figure 4. XRD patterns for SWNT/PANI composites with different SWNT content. Solid lines and dashed lines, respectively, denote the peaks of PANI and SWNT.

nanotubes consist of a graphitic sheet, which has been rolled up into a cylindrical shape. The π-bonded surface of the carbon nanotubes may interact strongly with the conjugated structure of polyaniline through π−π interactions.[24,25,28] In the present *in situ* polymerization process, the polyaniline could be considered to grow along the surface of SWNTs because of the strong π−π interactions between the two components. Meanwhile, the chain packing of polyanilines will also be ordered due to the template effect of 1D nanostructured CNTs. The following XRD and Raman spectra analyses confirmed this viewpoint.

As shown in Figure 4, the XRD patterns of the pure SWNTs exhibit four typical powder peak diffractograms at 2θ = 26.2, 28.4, 42.7, and 47.1°.[29] For the pure PANI, three broad peaks at 2θ = 15, 20, and 25° are assigned to the repeat unit of the polyaniline chain, the periodicity perpendicular to the polymer backbone chain, and periodicity parallel to the polymer backbone chain, respectively.[30] No obvious SWNT peaks were observed in the XRD pattern for the samples containing SWNTs less than 25 wt %. When we turn our attention to the change of polyaniline-related peaks, it was found that the full width at half-maximum (fwhm) of the main peak at 25° decreases from 0.82 to 0.71° when the SWNT content increases from 0 to 25 wt %. The peak sharpening usually relates to the monodistribution of the periodicity between the polymer backbone chains, suggesting that the molecular arrangement of polyaniline in the SWNT/PANI composite becomes ordered.

Raman spectra analysis (Figure 5) gives further evidence for the ordering of the PANI along the SWNT. The spectra of pure carbon nanotubes show a strong peak at 1588 cm^{-1}, assigned to the G band (in-plane stretching E_{2g} mode). For the pure PANI, C−H bending of the quinoid/benzenoid ring (~1162 cm^{-1}), weak C−N stretching (~1218 cm^{-1}), C═N stretching of the quinoid ring (~1483 cm^{-1}), and C−C stretching of the benzenoid rings (~1590 cm^{-1}) were observed.[31] It is worth noting that the peak intensities at 1483 and 1164 cm^{-1} in the composites decrease with the increase of SWNT content, while the peak intensity at 1590 cm^{-1} increases at the same time, suggesting a decrease in the quinoid unit concentration and an increase in the benzenoid unit concentration. Previous studies on the Raman characterization of carbon nanotubes (CNT)/PANI

TABLE 1. Characteristic Mott Temperature T_0, Carrier Mobility, and Carrier Density at Room Temperature for SWNT/PANI Composites

samples (wt %)	T_0 (10^3 K)	carrier mobility ($cm^2 V^{-1} s^{-1}$)	carrier density (10^{20} cm^{-3})
0.0	2.0	0.18	3.5
7.6	0.9	0.31	5.4
14.9	0.6	0.68	5.1
25	0.4	0.97	7.3

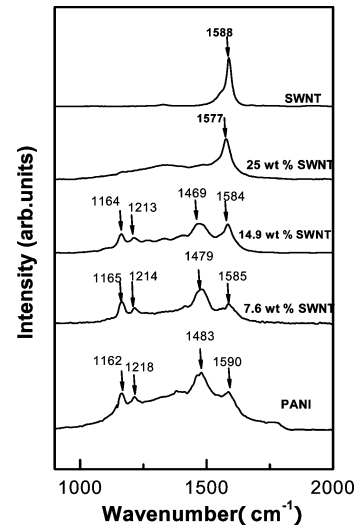

Figure 5. Raman spectra (λ_{exp} = 632.8 nm) for SWNT/PANI composites with different SWNT content.

suggested that the decrease of Raman peak intensities at 1164 and 1483 cm^{-1} results from the site-selective interactions (*i.e.*, $\pi-\pi$ conjugated) between the quinoid rings and carbon nanotubes,[32] which contributes to the chemical transformation of quinoid rings to benzenoid rings. Moreover, Silva *et al.* have studied the Raman characterization of polyaniline induced by the structure change of the polymer chain. They found that the peak intensity at 1483 cm^{-1} of polyaniline decreased, even vanished, when the conformation of polyaniline changes from a coil-like structure to an extended one.[33] As a result, in the present study, for SWNT/PANI composites, the decrease of Raman peak intensities at 1164 and 1483 cm^{-1} with increasing SWNT content is attributed to the site-selective interactions between the quinoid rings and carbon nanotubes, which induced the chemical transformation of quinoid rings to benzenoid rings and caused the conformational changes of polyaniline from a coil-like structure to an extended one. On the other hand, it was also found that all of the peaks at 1218, 1483, and 1590 cm^{-1} shift to the lower frequencies after addition of SWNTs, which may result from the additional $\pi-\pi$ conjugated interactions between the polyaniline and SWNTs that induce the red shift of Raman spectra.[24]

Accordingly, the obtained results support the following scenario: When SWNTs and aniline were mixed, the aniline molecules were absorbed to the surface of the nanotube by the formation of a charge-transfer complex.[26] After adding HCl and ammonium peroxidisulfate (APS), doped polyaniline was obtained by an oxidation polymerization reaction. The strong $\pi-\pi$ interactions between polyaniline and carbon nanotubes make polyaniline tightly coated on the SWNTs' surface. Then the absorbed PANIs grow along the hexagonal lattice of the SWNT, resulting in the expanded molecular conformation and a good order of chain packing. The ordered molecular structure not only reduces the $\pi-\pi$ conjugated defects in the polymer backbone due to ring twisting but also increases the effective degree of electron delocalization and therefore lowers the carrier hopping barrier.[4−6,14] Consequently, the carrier mobility in polyaniline was enhanced. In addition, the CNTs can also bridge the carrier transport by the strong $\pi-\pi$ interactions with the rings of polyaniline, which may further increase the carrier mobility. As a result, both electrical conductivity and Seebeck coefficient of composites are remarkably increased. Toshima has reported that the mechanical stretching could improve the chain ordering of polyaniline and therefore enhance the TE performance.[4,5] The present results provide a novel "chemical stretching" approach based on $\pi-\pi$ interaction to improve the chain ordering and TE performance of conducting polymers.

Compared with obvious improvement of electrical transport properties of the composites, the thermal conductivity was found to be insensitive to the addition of SWNTs. The experimental thermal conductivities are shown in Figure 6. For comparison, the calculated values according to particle mixture rule are also shown in Figure 6, and the thermal conductivity (35 W/m · K) of pure random SWNT material was used in calculating the thermal conductivity of SWNT/PANI.[34] It is clear that the thermal conductivities of the composites increase with SWNT content, but the increasing rate is much lower than the estimated values on the mixture rule. Even for the sample with 41.4 wt % SWNT, the thermal conductivity is still as low as 1.5 W/m · K, 1 order of magnitude lower than that of the calculated value. Such a low thermal conductivity can be compared with those of the currently best-known TE materials, such as Bi_2T_3-based alloys.[35] The total thermal conductivity (κ_{total}) for TE materials comprises electrical component (κ_e) and lattice component (κ_l), $\kappa_{total} = \kappa_e + \kappa_l$. The κ_e is estimated by Weidemann−Franz relation ($L_0\sigma T$) with a Lorentz constant of $L_0 = 2.45 \times 10^{-8}$ V^2/K^2. In SWNT/PANI composites, the electrical conductivity is low (10^3-10^4 S/m), and therefore, the proportion of κ_e to κ_{total} is very small (*e.g.*, only 6% for the sample with 41.4 wt % SWNT). The κ_{total} of the composites mainly depends on the κ_l. Previous theoretical and experimental investigations have indicated that the nanostructures, including nanoinclusions and nanointerfaces in composites, can scatter phonons and reduce κ_l.[36,37] In the present SWNT/PANI composites, the PANI(shell)−SWNT(core) nanostructures form a great amount of nanointerfaces, which may act as the effective scattering centers of phonons, and then decrease κ_l. The addition of SWNTs enhanced the carrier mobility in the ordered chain structures of the PANI and then increased the electrical conductivity as well as κ_e, but the κ_l was retained in a small amount of increase as compared with the value calculated by the normal mixture rule due to the additional scattering modes to phonons by nanostructures.

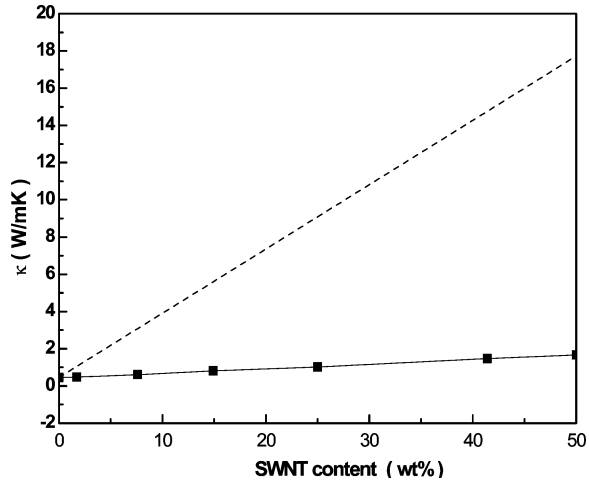

Figure 6. Thermal conductivity for SWNT/PANI composites with different SWNT content at room temperature. The dashed line is the calculated values based on particle mixture rule.

Finally, ZT values of the composites at room temperature were calculated. The maximum ZT at room temperature is estimated to be 0.004 for the composite with 41.4 wt % SWNT. So far, for conducting polymer-based composites, high ZT at 0.02 has been reported in film materials.[23] As for bulk materials, the ZT value of 0.004 obtained in the present work is among the best levels. It is expected to further improve the thermoelectric performance through further optimization of doping level and the microstructure of polyaniline.

CONCLUSIONS

In summary, the SWNT/PANI hybrid nanocable composites with ordered molecular structure have been prepared at room temperature by *in situ* polymerization. The XRD and Raman analysis results showed that the PANIs in the composite possess more ordered molecular structure than that of pure PANI, which may originate from the strong $\pi-\pi$ interactions between PANI and nanotubes. The ordered structures result in the increase of carrier mobility. Consequently, both electrical conductivity and Seebeck coefficient of the PANI-based polymer composite are dramatically improved as compared with pure PANI. The thermal conductivities of the composites, even with high SWNT content, do not change much and still keep very low values, which is attributed to the phonon scattering effect of nanointerfaces produced by the SWNT/PANI nanocable structure. The maximum power factor of the composites reaches 2×10^{-5} Wm^{-1} K^{-1}, and the ZT value reaches 0.004 at room temperature. Both of them are among the best bulk polymer-based composite TE materials. These results suggest that ordering the chain structure of conducting polymers *via* a chemical stretching approach is a novel and effective way for improving their thermoelectric performance.

MATERIALS AND METHODS

The nanocomposites were synthesized by one-step *in situ* polymerization of aniline (AR) with ammonium peroxidisulfate (APS) as the oxidant in the presence of SWNTs (SWNT wt % >90%, Timesnano, Co.). The SWNTs were 1−2 nm in diameter and about 30 μm in length. Aniline monomer was purified by vacuum distillation before reaction. A solution of 20 mL of 1 M HCl containing different masses (0, 0.1, 0.2, 0.3, 0.4, and 0.5 g) of SWNTs was sonicated at room temperature for 2 h. One milliliter of aniline monomer (1.0216 g/cm^3) was added to the suspension. The mixed solution was stirred for 30 min, and then 2 g of APS in 8 mL of 1 M HCl solution was slowly added dropwise to the well-stirred reaction mixture. After a few minutes, the dark suspension became green, indicating polymerization of aniline. The reaction was carried out at room temperature (30−35 °C) by stirring for 4 h. The products were filtered and washed with deionized water and alcohol and then dried under vacuum at 60 °C for 48 h. The SWNT contents are determined based on the initial weight of SWNTs and the total dry weight of composites.

X-ray powder diffraction (XRD) measurement was performed using a diffractometer (Rigaku RINT2000) with Cu Kα (λ = 0.15406 nm) radiation. Raman spectra were recorded on a JY LabRam-1B ($\lambda_{exc.}$ = 632.8 nm). The morphology was probed by transmission electron microscopy (JEM-2100F) (TEM) and scanning electron microscopy (JSM-6360LV) (SEM). The electrical conductivity and Seebeck coefficient were measured on the pressed powder pellet (relative density >90%) following the method previously reported.[6] The carrier concentration and carrier mobility measurements were performed in a Quantum Design Physics Property Measurement System (PPMS). The measurement of thermal diffusivity (λ) was performed by a laser flash method (Netzsch LFA 427), and specific heat (C_p) was studied with differential scanning calorimeters (PE DSC-2). The thermal conductivity was calculated from the relationship $\kappa = \rho\lambda C_p$, where ρ is the mass density.

Acknowledgment. This work was partially supported by the National Basic Research Program of China (973 Program, No. 2007CB607502), National Natural Science Foundation of China (Grant No. 50821004), The Science and Technology Commission of Shanghai Municipality (Grant Nos. 08DZ2210900 and 09XD1404400).

REFERENCES AND NOTES

1. Tritt, T. M.; Böttner, H.; Chen, L. D. Thermoelectrics: Direct Solar Thermal Energy Conversion. *MRS Bull.* **2008**, *33*, 366–367.
2. Snyder, G. J.; Toberer, E. S. Complex Thermoelectric Materials. *Nat. Mater.* **2008**, *7*, 105–114.
3. Toshima, N. Conductive Polymers as a New Type of Thermoelectric Material. *Macromol. Symp.* **2002**, *186*, 81–86.
4. Hiroshige, Y.; Ookawa, M.; Toshima, N. High Thermoelectric Performance of Poly(2,5-dimethoxyphenylenevinylene) and Its Derivatives. *Synyh. Met.* **2006**, *156*, 1341–1347.
5. Yan, L.; Ohta, N; Toshima, N. Streched Polyaniline Films Doped by (±)-10-Camphorsulfonic Acid: Anisotropy and Improvement of Thermoelectric Properties. *Macromol. Mater. Eng.* **2001**, *286*, 139–142.
6. Yao, Q.; Chen, L. D.; Xu, X. C.; Wang, C. F. The High Thermoelectric Properties of Conducting Polyaniline with Special Submicron-Fibre Sructure. *Chem. Lett.* **2005**, *34*, 522–523.
7. Yu, C.; Kim, Y. S.; Kim, D.; Grunlan, J. C. Thermoelectric Behavior of Segregated-Network Polymer Nanocomposites. *Nano Lett.* **2008**, *8*, 4428–4432.
8. Levesque, I.; Gao, X.; Klug, D. D.; Tse, J. S.; Ratcliffe, C. I.; Leclerc, M. Highly Soluble Poly(2,7-carbazolenevinylene) for Thermoelectrical Applications: From Theory to Experiment. *React. Funct. Polym.* **2005**, *65*, 23–36.
9. Liu, H.; Wang, J.; Hu, X. B.; Boughton, R. I.; Zhao, S. R.; Li, Q.; Jiang, M. H. Structure and Electronic Transport Properties of Polyaniline/$NaFe_4P_{12}$ Composite. *Chem. Phys. Lett.* **2002**, *352*, 185–190.
10. Lévesque, I.; Bertrand, P.; Blouin, N.; Leclerc, M.; Zecchin, S.; Zotti, G.; Ratcliffe, C. I.; Klug, D. D.; Gao, X.; Gao, F.; *et al.* Synthesis and Thermoelectric Properties of Polycarbazole, Polyindolocarbazole, and Polydiindolocarbazole Derivatives. *Chem. Mater.* **2007**, *19*, 2128–2138.
11. Makala, R. S.; Jagannadham, K.; Sales, B. C. J. Pulsed Laser Deposition of Bi_2Te_3-Based Thermoelectric Thin Films. *J. Appl. Phys.* **2003**, *94*, 3907–3918.
12. Liufu, S. C.; Chen, L. D.; Yao, Q; Wang, C. F. Assembly of One-Dimensional Nanorods into Bi_2S_3 Films with Enhanced Thermoelectric Transport Properties. *Appl. Phys. Lett.* **2007**, *90*, 112106.
13. Long, Y.; Chen, Z.; Zhang, X.; Zhang, J.; Liu, Z. Synthesis and Electrical Properties of Carbon Nanotube Polyaniline Composites. *Appl. Phys. Lett.* **2004**, *85*, 1796–1798.
14. MacDiamid, A. G.; Epstein, A. J. Secondary Doping in Polyaniline. *Synth. Met.* **1995**, *69*, 85–92.
15. Xia, Y. N.; Yang, P. D.; Sun, Y. G. One-Dimensional Nanostructures: Synthesis, Characterization, and Applications. *Adv. Mater.* **2003**, *15*, 353–389.

16. Hong, B. H.; Bae, S. C.; Lee, C.; Jeong, S.; Kim, K. S. Ultrathin Single-Crystalline Silver Nanowire Arrays Formed in an Ambient Solution Phase. *Science* **2001**, *294*, 348–351.
17. Nicewarner-Pena, S. R.; Freeman, R. G.; Reiss, B. D.; He, L.; Pena, D. J.; Walton, I. D.; Cromer, R.; Keating, C. D.; Natan, M. J. Submicrometer Metallic Barcodes. *Science* **2001**, *294*, 137–141.
18. Zach, M. P.; Ng, K. H.; Penner, R. M. Molybdenum Nanowires by Electrodeposition. *Science* **2000**, *290*, 2120–2123.
19. Zhang, Y.; Dai, H. Formation of Metal Nanowires on Carbon Nanotubes. *Appl. Phys. Lett.* **2000**, *77*, 3015–3017.
20. Ajayan, P. M.; Stephan, O.; Redlich, P.; Colliex, C. Carbon Nanotubes as Removable Templates for Metal Oxide Nanocomposites ANS Nanostructures. *Nature* **1995**, *375*, 564–567.
21. O'Connell, M. J.; Boul, P.; Ericson, L. M.; Huffman, C.; Wang, Y.; Haroz, E.; Kuper, C.; Tour, J.; Ausman, K. D.; Smalley, R. E. Reversible Water-Solubilization of Single-Walled Carbon Nanotubes by Polymer Wrapping. *Chem. Phys. Lett.* **2001**, *342*, 265–271.
22. Balavoine, F.; Schultz, P.; Richard, C.; Mallouh, V.; Ebbsen, T. W.; Mioskowski, C. Helical Crystallization of Proteins on Carbon Nanotubes: A First Step towards the Development of New Biosensors. *Angew. Chem., Int. Ed.* **1999**, *38*, 1912–1915.
23. Kim, D.; Kim, Y.; Choi, K.; Grunlan, J. C.; Yu, C. Improved Thermoelectric Behavior of Nanotube-Filled Polymer Composites with Poly(3,4-ethylenedioxythiophene) Poly(styrenesulfonate). *ACS Nano* **2010**, *4*, 513–523.
24. Zengin, H; Zhou, W.; Jin, J.; Czerw, R.; Smith, D. W., Jr. Carbon Nanotube Doped Polyaniline. *Adv. Mater.* **2002**, *14*, 1480–1483.
25. Sainz, R.; Benito, A. M.; Martínez, M. T.; Galindo, J. F. Soluble Self-Aligned Carbon Nanotube/Polyaniline Composites. *Adv. Mater.* **2005**, *17*, 278–281.
26. Sun, Y.; Wilson, S. R.; Schuster, D. I. High Dissolution and Strong Light Emission of Carbon Nanotubes in Aromatic Amine Solvents. *J. Am. Chem. Soc.* **2001**, *123*, 5348–5349.
27. Meng, C. Z.; Liu, C. H.; Fan, S. S. A Promising Approach to Enhanced Thermoelectric Properties Using Carbon Nanotube Networks. *Adv. Mater.* **2010**, *22*, 535–539.
28. Chen, R. J.; Zhang, Y.; Wang, D.; Dai, H. Noncovalent Sidewall Functionalization of Single-Walled Carbon Nanotubes for Protein Immobilization. *J. Am. Chem. Soc.* **2001**, *123*, 3838–3839.
29. Zhou, O.; Fleming, R. M.; Murphy, D. W.; Chen, C. H.; Haddon, R. C.; Ramirez, A. P.; Glarum, S. H. Defects in Carbon Nanostructures. *Science* **1994**, *263*, 1744–1747.
30. Pouget, J. P.; Jozefowicz, M. E.; Epstein, A. J.; Tang, X.; MacDiarmid, A. G. X-ray Structure of Polyaniline. *Macromolecules* **1991**, *24*, 779–789.
31. Cochet, M.; Louarn, G.; Quillard, S.; Buisson, J. P.; Lefrant, S. Theoretical and Experimental Vibrational Study of Emeraldine in Salt Form. Part II. *J. Raman Spectrosc.* **2000**, *31*, 1041–1049.
32. Pereira da Silva, J. E.; Córdoba de Torresi, S. I.; de Fria, D. L. A.; Temperini, M. L. A. Raman Characterization of Polyaniline Induced Conformational Changes. *Synth. Met.* **1999**, *101*, 834–835.
33. Cochet, M.; Maser, W. K.; Benito, A. M.; Callejas, A.; Martínez, M. T.; Benoit, J. M.; Schreiberb, J.; Chauvet, O. Synthesis of a New Polyaniline/Nanotube Composite: "In-Situ" Polymerization and Charge Transfer through Site-Selective Interaction. *Chem. Commun.* **2001**, 1450–1451.
34. Hong, J.; Llaguno, M. C.; Nemes, N. M. Electrical and Thermal Transport Properties of Magnetically Aligned Single Wall Carbon Nanotube Films. *Appl. Phys. Lett.* **2000**, *77*, 666–668.
35. Jiang, J.; Chen, L. D.; Bai, S. Q.; Yao, Q.; Wang, Q. Thermoelectric Properties of Textured p-Type $(Bi, Sb)_2Te_3$ Fabricated by Spark Plasma Sintering. *Scripta Mater.* **2005**, *52*, 347–351.
36. Minnich, A. J.; Dresselhaus, M. S.; Ren, Z. F.; Chen, G. Bulk Nanostructured Thermoelectric Materials: Current Research and Future Prospects. *Energy Environ. Sci.* **2009**, *2*, 466–479.
37. Sootsman, J. R.; Kong, H.; Uher, C.; D'Angelo, J. J.; Wu, C. I.; Hogan, T. P.; Caillat, T.; Kanatzidis, M. G. Large Enhancements in the Thermoelectric Power Factor of Bulk PbTe at High Temperature by Synergistic Nanostructuring. *Angew. Chem., Int. Ed.* **2008**, *47*, 1–6.